Supporting Information

Probing Comonomer Selection Effects on Dioxythiophene-Based Aqueous Compatible Polymers for Redox Applications

Abigail A. Advincula[a], Austin L. Jones[b], Karl J. Thorley[c], Anna M. Österholm[b], James F. Ponder Jr.[d], and John R. Reynolds[a,b*]

[a]*School of Materials Science and Engineering, Georgia Institute of Technology, Atlanta, GA 30332, USA*

[b]*School of Chemistry and Biochemistry, Georgia Institute of Technology, Atlanta, GA 30332, USA*

[c]*Center for Applied Energy Research, University of Kentucky, Lexington, KY 40511, USA*

[d]*George W. Woodruff School of Mechanical Engineering, Georgia Institute of Technology, Atlanta, GA 30332, USA*

*E-mail: reynolds@chemistry.gatech.edu

Materials

All starting materials were purchased from a commercial supplier and were used without further purification. Starting monomers ProDOT(OE3), dibromo-EDOT, dibromo-PheDOT and dibromo-dimethyl-ProDOT were prepared using published methods.[1–3] All polymerizations were carried out in dry and degassed HPLC grade DMAc. Silica gel used for column chromatography was purchased from Sorbent Technologies, Inc (60 Å porosity).

Instrumentation & Measurement Details

^{1}H NMR for all polymers were acquired on a Bruker 400 MHz instrument using deuterated chloroform ($CDCl_3$) at 50 °C; the residual $CHCl_3$ peak was used as a reference for all reported polymer chemical shifts (^{1}H: δ= 7.28 ppm). Gel permeation chromatography (GPC) was performed with a Tosoh EcoSEC system equipped with an RI detector at a 1 mg/mL flow rate to determine the number average molecular weight (M_n), weight average molecular weight (M_w) and dispersity (Đ) for all polymers relative to polystyrene standards at 40 °C in $CHCl_3$. All elemental analyses were conducted by Atlantic Microlab Inc.

Films for QCM-D measurements were spray-cast onto gold-coated 5 MHz quartz crystals (Gold QSensors -QSX 301) from NanoScience Instruments. Prior to casting, the gold surface of the quartz crystals was UV-ozone treated for 10 minutes; cleaned with sodium dodecyl sulfate solution, deionized (DI) water and toluene with thorough drying under argon after the DI water and toluene steps; and then UV-ozone treated again for 10 minutes. Films were then spray-cast onto the Gold QSensors using an Iwata-Eclipse HP-BC airbrush with argon (20 psi) as the carrier gas. The thicknesses of films used for QCM-D were determined using a Bruker DektakXT profilometer. QCM-D measurements were taken on a Q-Sense Analyzer system (Biolin Scientific AB, Sweden) to study the swelling from a dry film to fully swollen in 0.5 M NaCl in MilliPore water. The experiments were performed at room temperature with a flow rate of 0.1 mL/min using a peristaltic pump.

All electrochemical experiments were performed under inert atmosphere and with thoroughly purged electrolyte solutions. The electrolytes used included 0.5 M NaCl dissolved in DI water and 0.5 M tetrabutylammonium hexafluorophosphate ($TBAPF_6$, Acros Organics, 98%, recrystallized from hot ethanol) dissolved in propylene carbonate. A platinum flag served as the counter electrode. For measurements performed in aqueous electrolyte, a Ag/AgCl (3M NaCl, BASi Inc.) was used as the reference electrode. For measurements in 0.5 M $TBAPF_6$/PC, a AgCl coated silver wire pseudo-reference electrode (calibrated vs. Fc/Fc^+, $E_{1/2}$ = 0.39 V) was used.

The redox behavior of the films was characterized using cyclic voltammetry and differential pulse voltammetry, which were performed in a three-electrode cell using an EG&G Princeton Applied Research 273A potentiostat/galvanostat, under CorrWare control. A glassy carbon working electrode (7 mm^2), was polished with 0.1 and 0.05 μm alumina powder and rinsed rigorously with water before use. Polymers were dissolved at 4 mg/mL in chloroform and 2 μL was drop cast (total deposited amount of 8 μg) onto the glassy carbon electrodes in 1 μL aliquots and left to dry at room temperature. Knowing the surface area of the glassy carbon electrode (0.07 cm^2) and assuming a density of 1.1 g/cm^3,[4] a film thickness of ~1 μm is estimated.

Solution UV-Vis and thin film absorption spectra were obtained on an Agilent Cary 5000 spectrophotometer in 1 cm path length quartz cuvettes scanning from 300-1350 nm. For these measurements, films were spray-cast to an optical density of 1.1 ± 0.1 (~200 nm) onto ITO/glass substrates (7 mm x 50 mm, 8-12 Ω/sq, Delta Technologies Ltd) using an Iwata-Eclipse HP-BC airbrush with argon (20 psi) as the carrier gas. Prior to the spectroelectrochemical measurements, polymer films were cycled (10x) between -0.7 to +0.8 V vs. Ag/AgCl in 0.5 M $NaCl/H_2O$ and -1.1 to +0.6 V vs. Fc/Fc^+ in 0.5 M $TBAPF_6$/PC.[5] Chronoabsoprtometry was measured by monitoring at the absorbance at λ_{max} as a function of switching rate with an Ocean Optics USB2000+ spectrophotometer detector using an Ocean Optics DH-2000-BAL fiber-optic light source. Photography was performed using a Nikon D90 SLR camera with a Nikon 18-105 mm VR lens in a photobooth under D50 illumination. The photographs are presented without any manipulation apart from cropping. The colors of the P(OE3) films were quantified by converting the absorbance spectra to CIELAB *L*a*b** color coordinates relative to CIE standard illuminant D50 where the *L** represent the white-black balance, *a** the green-red balance, and *b** the blue-yellow balance of a given color.

Films for *in-situ* conductance measurements were spray-cast onto interdigitated gold microelectrodes (Micrux technologies, ED-IDA1-Au) using an Iwata-Eclipse HP-BC airbrush with argon (20 psi) as the carrier gas, with films sprayed to ~200 nm. The data recorded using a Pine Bipotentiostat controlled by the Aftermath software. Experiments in 0.5 M $NaCl/H_2O$ were carried out in a three-electrode set-up using a Pt flag as the counter electrode, a Ag/AgCl (3M NaCl) electrode as the reference, and the polymer-coated IDE as the working electrode. Experiments performed in 0.5 M $TBAPF_6$/PC used a similar set-up, but with a Ag/AgCl wire pseudoreference (0.39 V vs. Fc/Fc^+) as the reference. Measurements are carried out on polymer-coated interdigitated microelectrodes where the *i-V* curve is recorded as one half of the electrodes are held at a constant direct current (DC) potential (working electrode 1, WE1) and the potential at the other electrode (working electrode 2, WE2) is scanned ±5 mV relative to WE1 at 0.5 mV/s.[6] From these recorded *i-V* curves, we subsequently extracted conductance values from linear fits of the slopes.

To build Type I supercapacitors, films (2 μL of 4 mg/mL solution drop-cast on the electrode surface in 1 μL aliquots) were prepared on glassy carbon electrodes (0.07 cm^2). Prior to device assembly, films were cycled (10x) at between -0.7 to +0.8 V vs. Ag/AgCl in 0.5 M $NaCl/H_2O$ to electrochemically condition the films. Then one film was electrochemically reduced at -0.7 V, and the other film was oxidized at +0.8 V for 30 s. An electrolyte-soaked cellulose separator separated the polymer-coated glassy carbon current

collectors. All electrochemical measurements were performed on a PAR273A potentiostat/galvanostat under CorrWare control.

Synthetic procedures for P(OE3)-D, P(OE3)-E, P(OE3)-Ph

A vessel of pre-dried DMAc, sitting over activated 4 Å molecular sieves, was purged with argon for 2 hours before each polymerization. A dry 100 mL round bottom flask was equipped with a magnetic stir bar, ProDOT(OE3), the corresponding dibromo monomer, 2% palladium acetate, ~ 0.3 equivalents of pivalic acid, and 2.5 equivalents of potassium carbonate. The round bottom was transferred into a glove box where it was sealed. The round bottom was removed from the glove box and the degassed DMAc was syringed into it. The mixture was allowed to stir at room temperature for 5 minutes and then lowered into a pre-heated, 30 °C-oil bath and ramped to 120 °C at a rate of 10 °C/ 5 minutes. The polymerization was allowed to proceed for 14 hours. Then the reaction was cooled to 90 °C and exposed to air to add an excess amount of palladium scavenger diethylammonium diethyldithiocarbamate, a potassium scavenger 18-crown-6, and 10 mL of chlorobenzene. The mixture was stirred for 1 hour before it was precipitated into 250 mL of methanol. The impure polymer was filtered through a cellulose extraction thimble and subjected to successive Soxhlet extractions with methanol, acetone, hexanes, THF, and finally isolated in chloroform. The chloroform solution was concentrated under reduced pressure, precipitated into methanol, collected via vacuum filtration, and dried under vacuum for 24 hours.

P(OE3)-D

ProDOT(OE3) (881 mg, 1.73 mmol), dibromo-dimethyl-ProDOT (592 mg, 1.73 mmol), $Pd(OAc)_2$ (8 mg, 0.036 mmol), 0.3 equivalents of pivalic acid (53 mg, 0.127 mmol), 2.5 equivalents of potassium carbonate (600 mg, 4.34 mmol), and 14 mL of DMAc were used. The mixture was allowed to stir at room temperature for 5 minutes and then lowered into a pre-heated, 30 °C-oil bath and ramped to 120 °C at a 10 degree every 5-minute rate. Then the reaction was cooled to 90 °C and exposed to air to add an excess amount of palladium scavenger diethylammonium diethyldithiocarbamate, a potassium scavenger 18-crown-6, and 10 mL of chlorobenzene. The polymer was collected in the chloroform Soxhlet fraction as a dark purple solid (900 mg, 76%). M_n: 27 kg/mol, M_w: 78.3 kg/mol, $Đ$: 2.9 (in chloroform at 40 °C vs. polystyrene). ^{1}H NMR (400 MHz, $CDCl_3$, 50 °C): δ (ppm) 4.20 (s, 4H), 3.87 (s, 4H), 3.76-3.60 (m, 24H), 3.55-2.50 (m, 4H), 3.36 (s, 6H), 1.17 (s, 6H). Anal. calcd. for $C_{32}H_{48}O_{12}S_2$: C (55.80%), H (7.02%), S (9.31%); Found: C (55.65%), H (6.94%), S (9.24%).

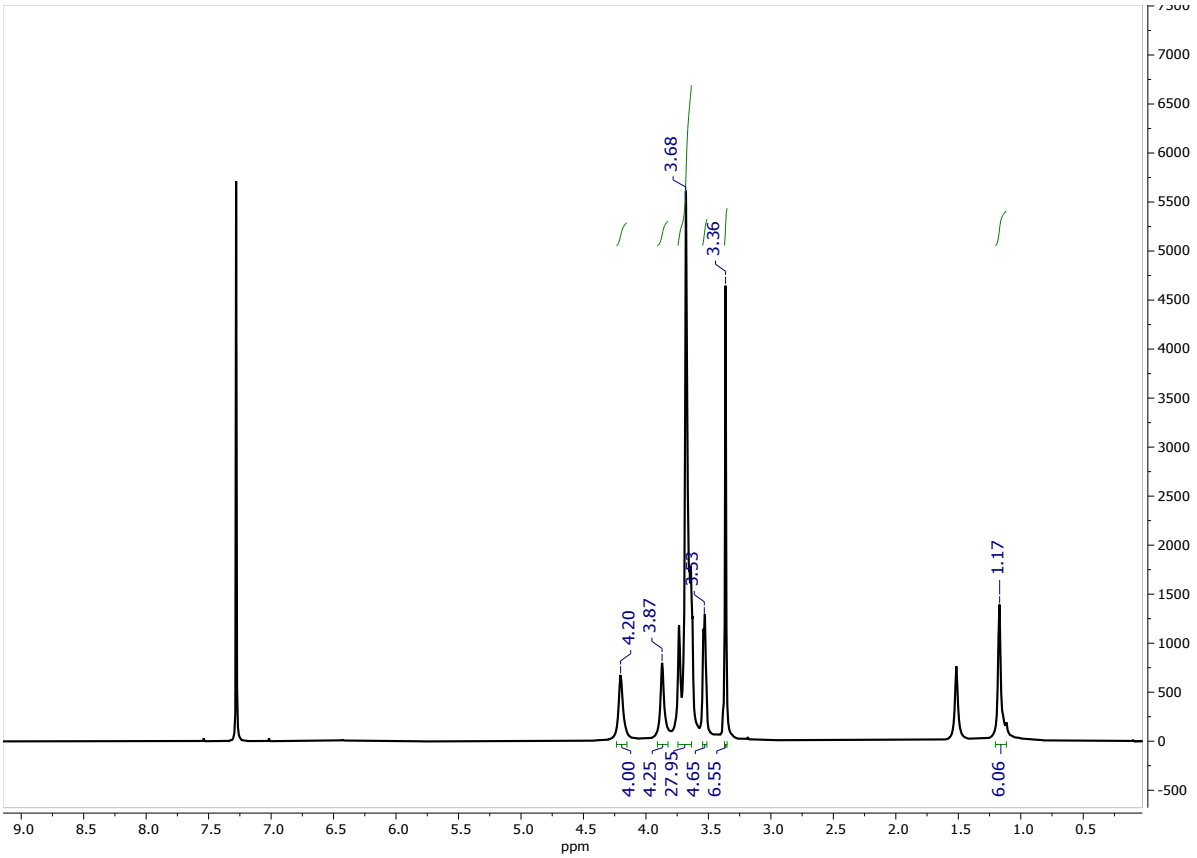

Figure S1. P(OE3)-D ^{1}H NMR in $CDCl_3$.

P(OE3)-E

ProDOT(OE3) (758 mg, 1.49 mmol), dibromo-EDOT (446 mg, 1.49 mmol), $Pd(OAc)_2$ (7 mg, 0.031 mmol), 0.3 equivalents of pivalic acid (45 mg, 0.44 mmol), 2.5 equivalents of potassium carbonate (515 mg, 3.73 mmol), and 10 mL of DMAc were used. The mixture was allowed to stir at room temperature for 5 minutes and then lowered into a pre-heated, 30 °C-oil bath and ramped to 120 °C at a 10 degree every 5-minute rate. Then the reaction was cooled to 90 °C and exposed to air to add an excess amount of palladium scavenger diethylammonium diethyldithiocarbamate, a potassium scavenger 18-crown-6, and 10 mL of chlorobenzene. The polymer was collected in the chloroform Soxhlet fraction as a dark purple solid (850 mg, 88%). M_n: 13 kg/mol, M_w: 26 kg/mol, $Đ$: 2.0 (in chloroform at 40 °C vs. polystyrene). ^{1}H NMR (400 MHz, $CDCl_3$, 50 °C): δ (ppm) 4.42 (s, 4H), 4.21 (s, 4H), 3.80-3.45 (m, 28H), 3.43-2.29 (m, 6H). Anal. calcd. for $C_{29}H_{42}O_{12}S_2$: C (53.86%), H (6.55%), S (9.91%); Found: C (53.13%), H (6.58%), S (9.85%).

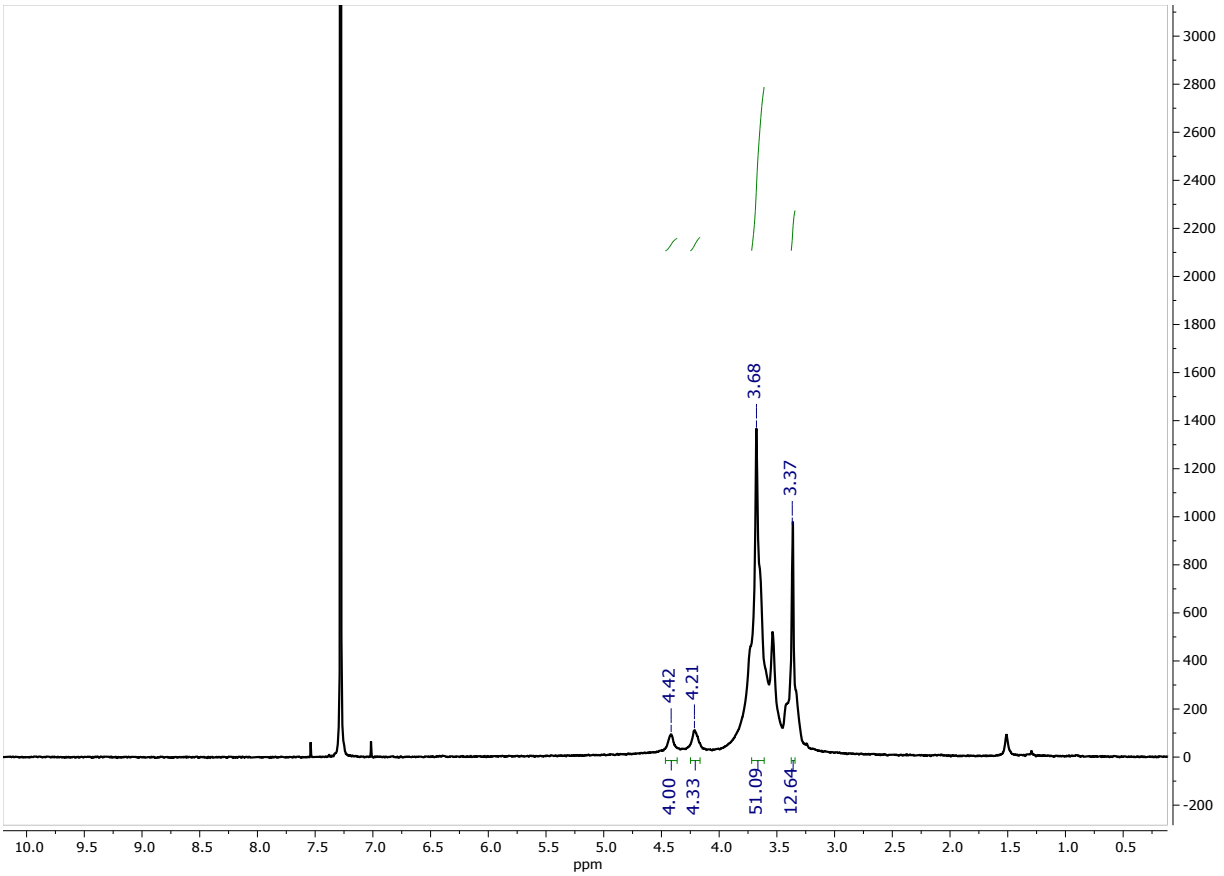

Figure S2. P(OE3)-E ^{1}H NMR in $CDCl_3$.

P(OE3)-Ph

ProDOT(OE3) (423 mg, 0.831 mmol), dibromo-PheDOT (290 mg, 0.833 mmol), $Pd(OAc)_2$ (4 mg, 0.18 mmol), 0.3 equivalents of pivalic acid (25 mg, 0.245 mmol), 2.5 equivalents of potassium carbonate (287 mg, 2.08 mmol), and 5 mL of DMAc were used. The mixture was allowed to stir at room temperature for 5 minutes and then lowered into a pre-heated, 30 °C-oil bath and ramped to 120 °C at a 10 degree every 5-minute rate. Then the reaction was cooled to 90 °C and exposed to air to add an excess amount of palladium scavenger diethylammonium diethyldithiocarbamate, a potassium scavenger 18-crown-6, and 10 mL of chlorobenzene. The polymer was collected in the chloroform Soxhlet fraction as a dark purple solid (400 mg, 70%). M_n: 19.9 kg/mol, M_w: 83.58 kg/mol, $Đ$: 4.2 (in chloroform at 40 °C vs. polystyrene). ^{1}H NMR (400 MHz, $CDCl_3$, 50 °C): δ (ppm) 7.16-6.90 (m, 4H), 4.27 (s, 4H), 4.00-3.48 (m, 28H), 3.42-3.30 (m, 6H). Anal. calcd. for $C_{33}H_{42}O_{12}S_2$: C (57.05%), H (6.09%), S (9.23%); Found: C (56.79%), H (5.90%), S (9.10%).

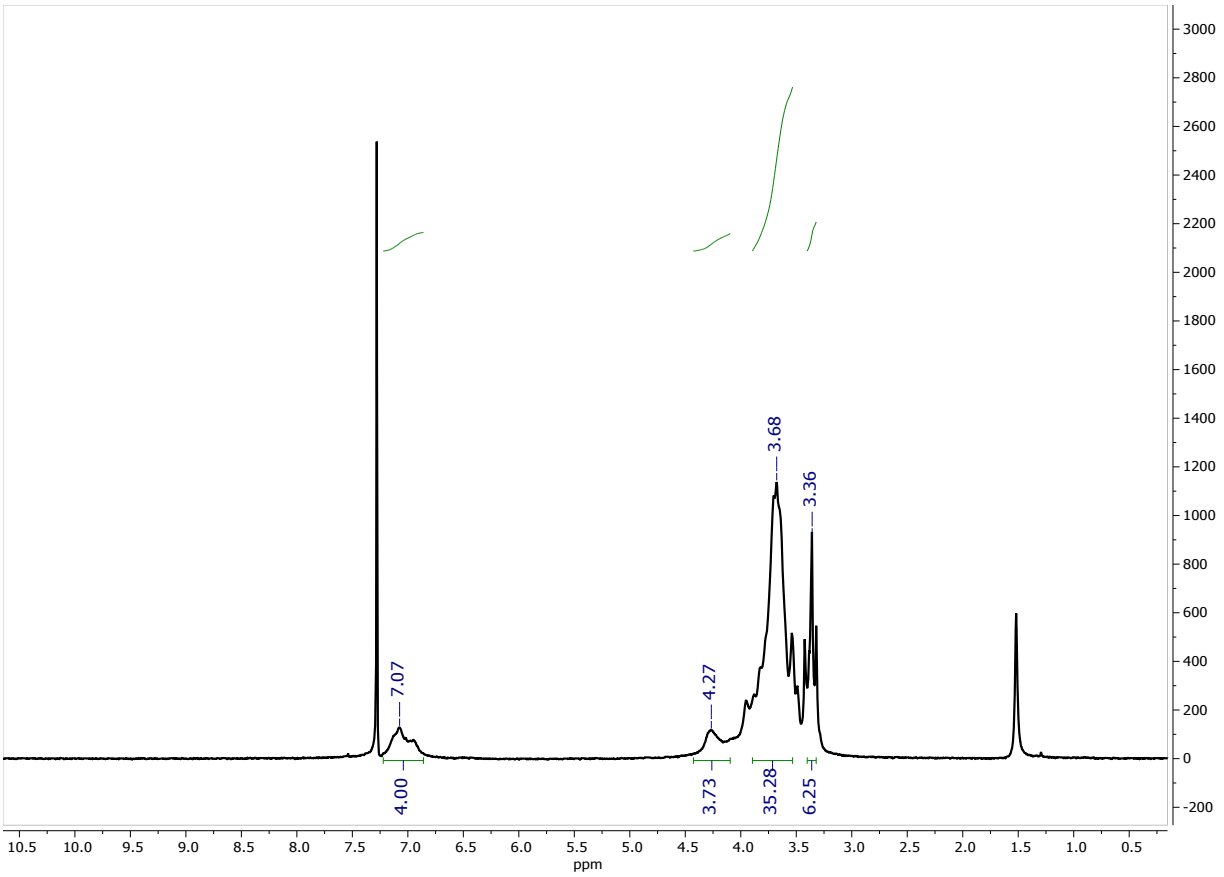

Figure S3. P(OE3)-Ph ^{1}H NMR in $CDCl_3$.

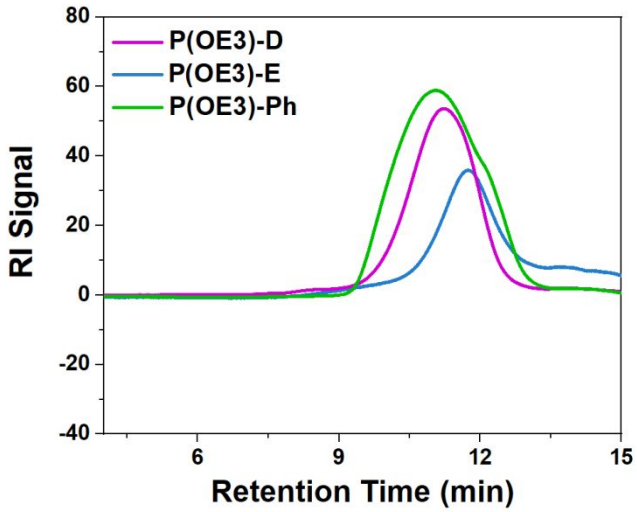

Figure S4. GPC traces using $CHCl_3$ as the eluent at 40 °C, at flow rate of 1 mg/mL.

Optical properties

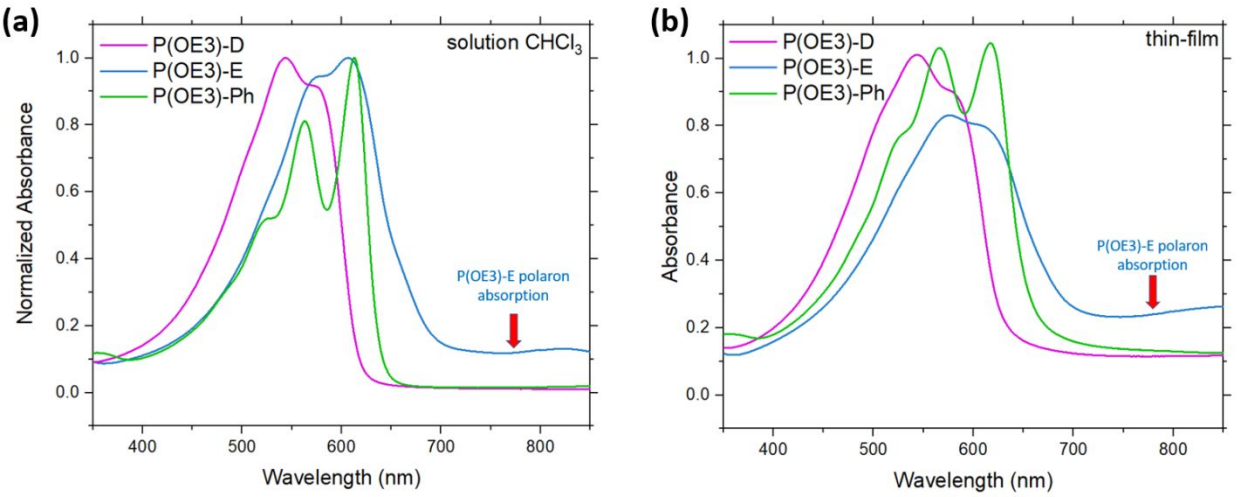

Figure S5. (a) Polymer solution spectra at a concentration of 0.02 mg/mL in chloroform. (b) Absorption spectra of spray-cast films (from a 4 mg/mL solution in $CHCl_3$, cast to an optical density of 1± ~0.1 on ITO/glass) in the as-cast state.

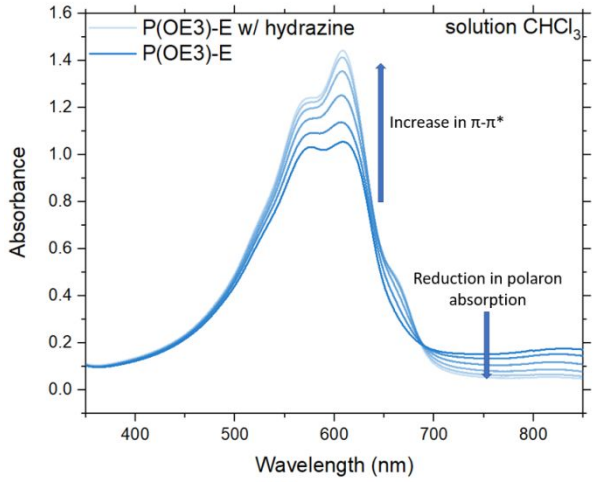

Figure S6. The effect of hydrazine reduction on the optical properties of P(OE3)-E in chloroform.

QCM-D Data

Electrolyte was flowed simultaneously over the three spray cast films on quartz chips and a bare quartz chip. Upon the introduction of electrolyte, the changes in dissipation (ΔD) and oscillation frequency (Δf) were monitored over 3.5 hours (**Figure S7**).

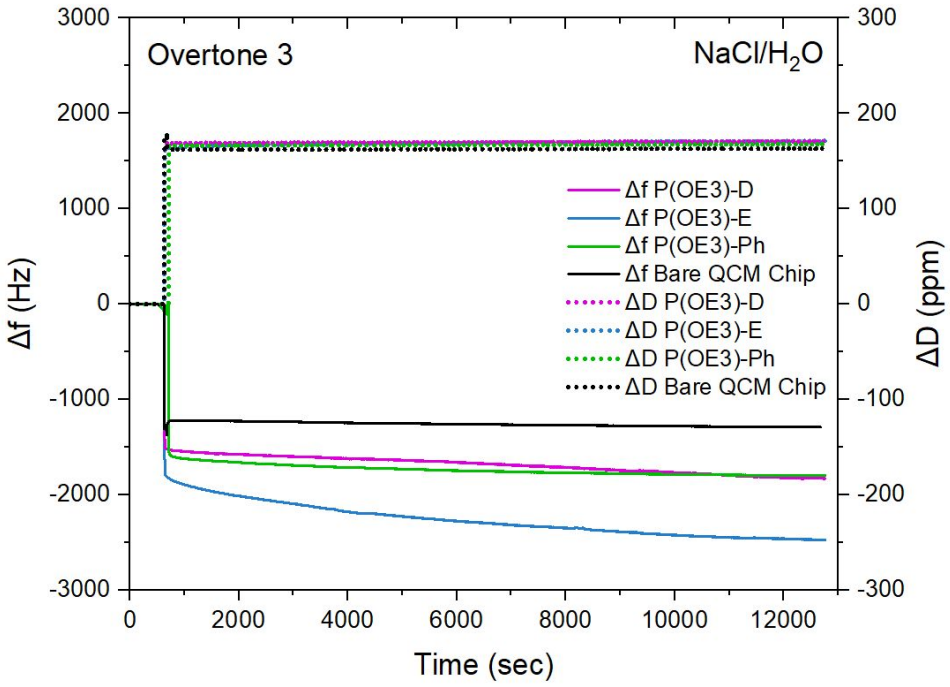

Figure S7. Passive swelling kinetics (changes in frequency and dissipation) of all copolymers in 0.5 M NaCl/H_2O as measured by QCM-D. Overtone 3 is shown. Film thickness ~140 ± 15 nm.

As there was little change in ΔD when comparing the bare chip to the chip with sprayed film, we surmised that the P(OE3) films behaved as rigid films under these conditions and that the Sauerbrey equation (**Equation S1**), which relates change in mass (Δm) to change in frequency (Δf),[7] could be used as an approximation. Furthermore, all polymers fell below a suggested threshold [8] of $|\Delta D_n/(\Delta f_n/n)| << 4 \times 10^{-7}$ Hz^{-1}.

$$\Delta m = -C\left(\frac{\Delta f}{n}\right)$$

Equation S1. The Sauerbrey equation.

The drop in frequency (Δf) observed in all samples (**Figure S7**) indicated an increase in mass (Δm), upon introduction of electrolyte. For the Δf of the polymer-coated quartz chips, we consider contributions from: (1) electrolyte flow over the chip and (2) electrolyte uptake of the polymer film. To extract the Δf due to electrolyte uptake of the polymer film, raw Δf data of the bare quartz chip was subtracted from raw Δf data for the polymer films.

This reduced Δf data ($\Delta f_{P(OE3)\text{-}x} - \Delta f_{\text{bare quartz}}$) was multiplied by the negative mass sensitivity constant (C) (for a 5 MHz crystal is 17.7 ng/cm^2) and divided by the harmonic (n, here we use the third overtone).

The Sauerbrey equation (**Equation S1**) was employed to extract the change in areal mass (Δm) in units of ng/cm^2 as a function of swelling time (**Figure S8a**). Implied changes in film thickness were calculated by dividing the areal mass by an assumed polymer density of 1.15 g/cm^3 (**Figure S8b**);[4] these values were then divided by the measured thickness of the dry films (140 ± 15 nm) to calculate the percent swelling (**Figure S8c**).[9]

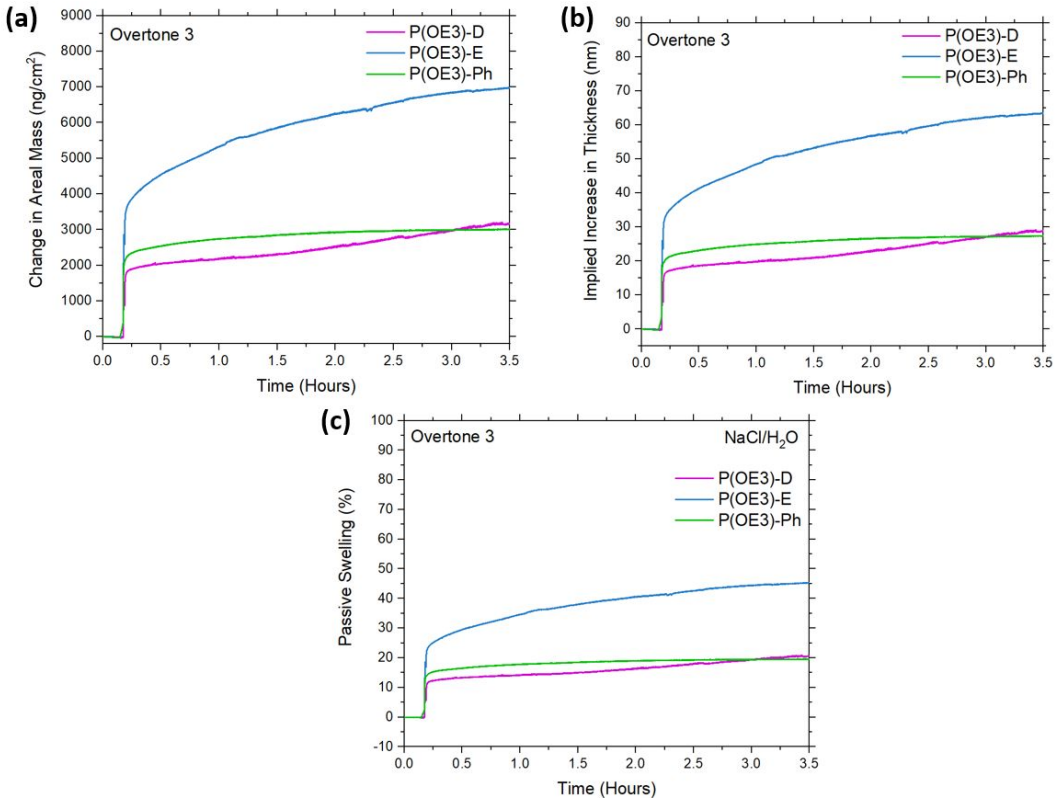

Figure S8. (a) Changes in areal mass as a function of time. (b) Changes in implied increase in thickness as a function of time. (c) Changes in swelling % as a function of time. Measurements done in 0.5 M NaCl/H_2O.

Electrochemical Measurements

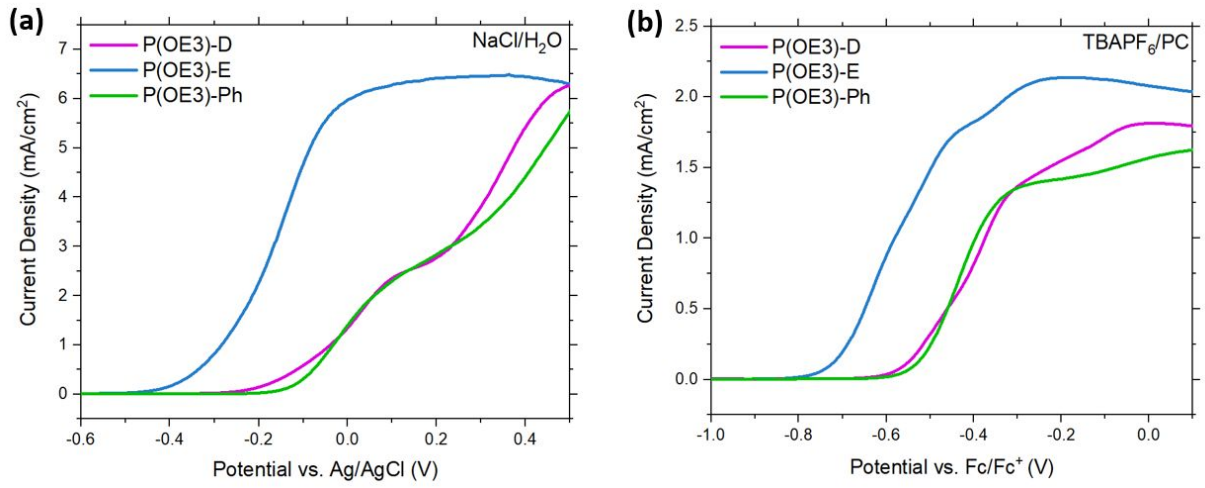

Figure S9. Differential pulse voltammograms of P(OE3) polymers in (a) 0.5 M $NaCl/H_2O$ and (b) 0.5 M $TBAPF_6$/PC (step size 2 mV, step time 0.1 s, and pulse time 0.02 s).

Density Functional Theory Computational Details

All calculations were run using Gaussian 16 Rev A.03[10] and NBO 6.0[12] Polymers were modeled as 12 repeating thiophene units, and geometries were optimized in the gas phase using ωB97XD/6-31G* where the range separation factor ω was set to 0.1 as a representative value for conjugated polymers. At the minimized geometry, the optimal ω value was found such that Koopmans' theorem was best described using a protocol described in previous work.[13] All subsequent calculations used this optimized ω value. Solvent was modelled using a self-consistent reaction field polarizable continuum.

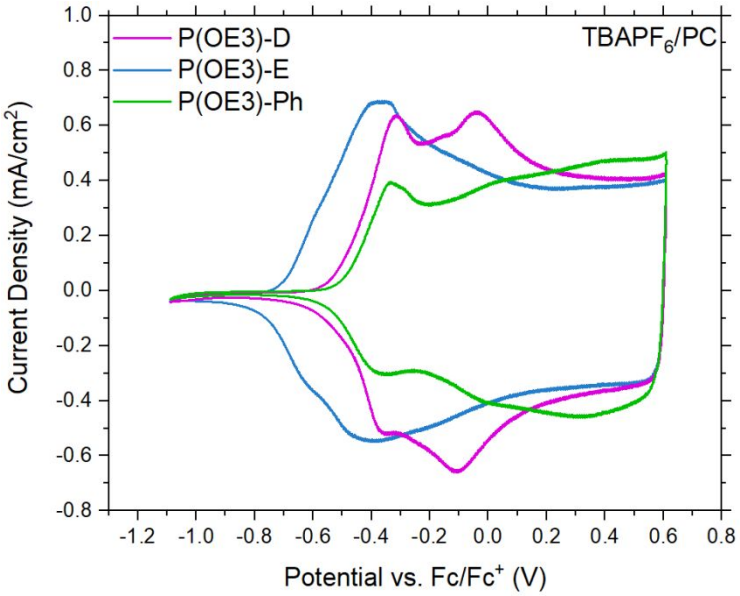

Figure S10. (a) Cyclic voltammograms of P(OE3) polymers measured at a scan rate of 50 mV/s on a glassy carbon button electrode in 0.5 M $TBAPF_6$/PC.

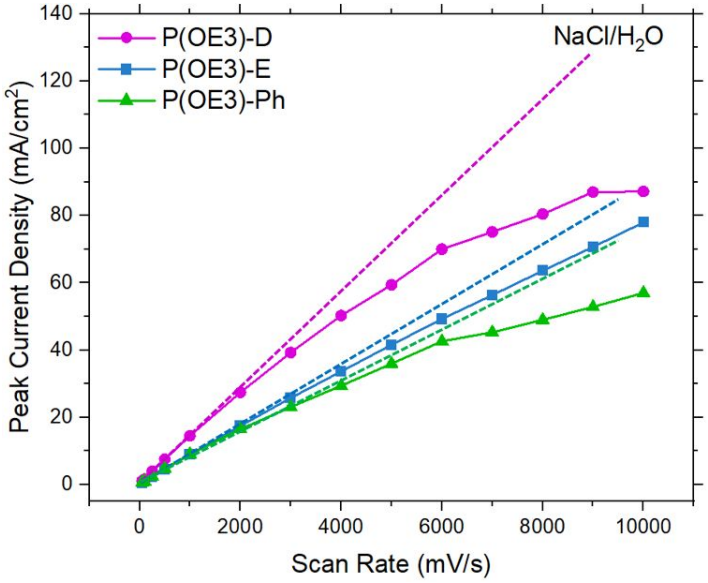

Figure S11. Peak current as a function of scan rate for P(OE3) series to 10 V/s. All measurements done in 0.5 M $NaCl/H_2O$ from -0.7 to +0.8 V vs. Ag/AgCl. Dashed lines indicate extrapolated linear fit for first four points.

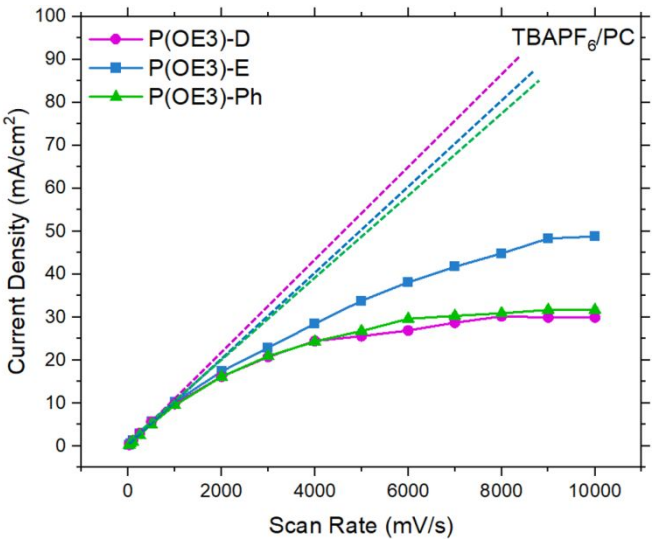

Figure S12. Peak current as a function of scan rate for P(OE3) series to 10 V/s. All measurements done in 0.5 M $TBAPF_6$/PC from -1.1 to +0.6 V vs. Fc/Fc^+. Dashed lines indicate extrapolated linear fit for first four points.

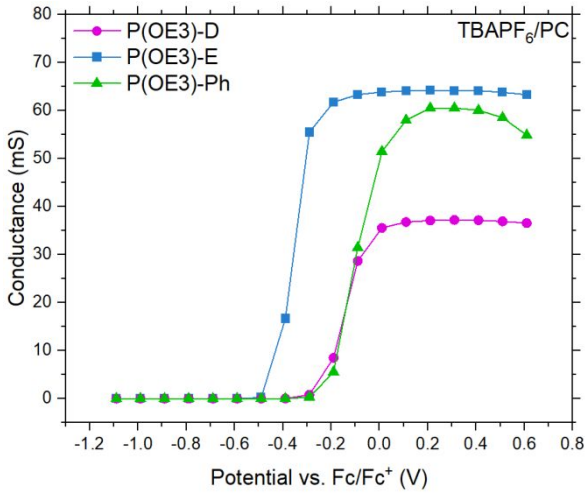

Figure S13. Potential-dependent conductance of the P(OE3) series in 0.5 M $TBAPF_6$/PC vs. Fc/Fc^+. Second forward scans are plotted.

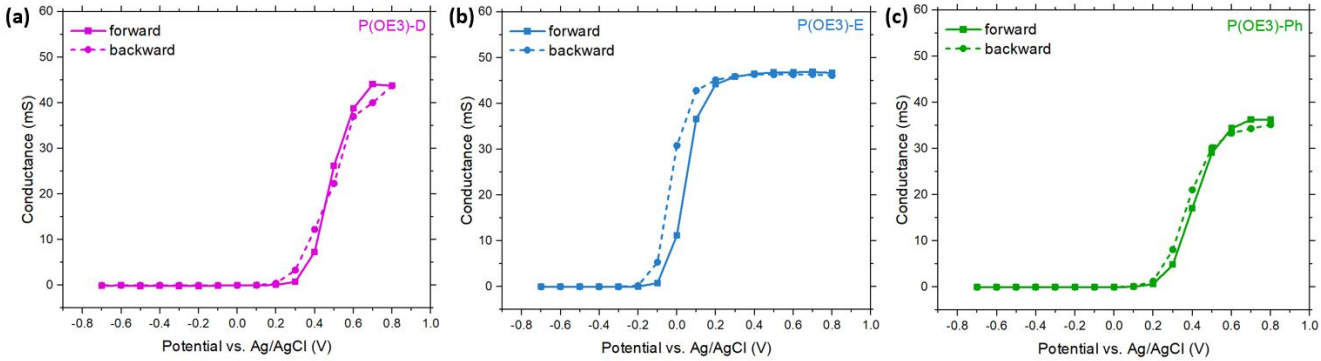

Figure S14. Forward and backward in-situ conductance scans of P(OE3) polymer series in 0.5 M NaCl/H_2O from -0.7 to +0.8 V vs. Ag/AgCl.

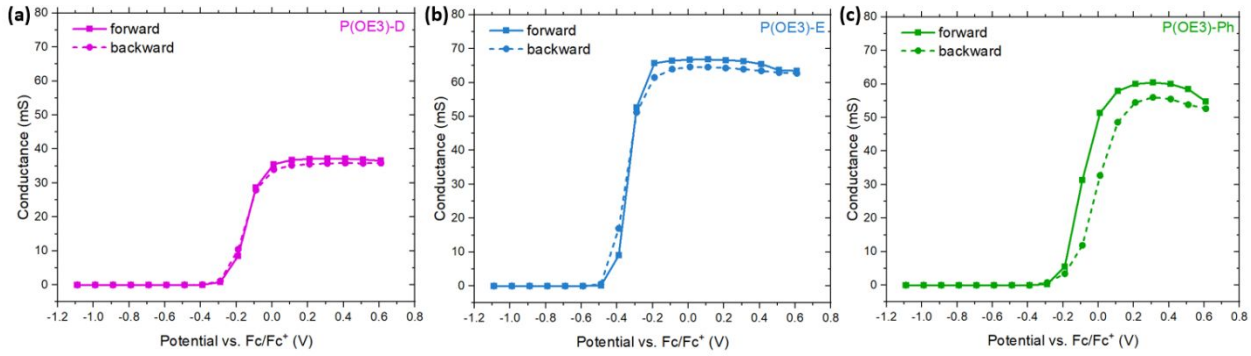

Figure S15. Forward and backward in-situ conductance scans of P(OE3) polymer series in 0.5 M $TBAPF_6$/PC from -1.1 to +0.6 V vs. Fc/Fc^+.

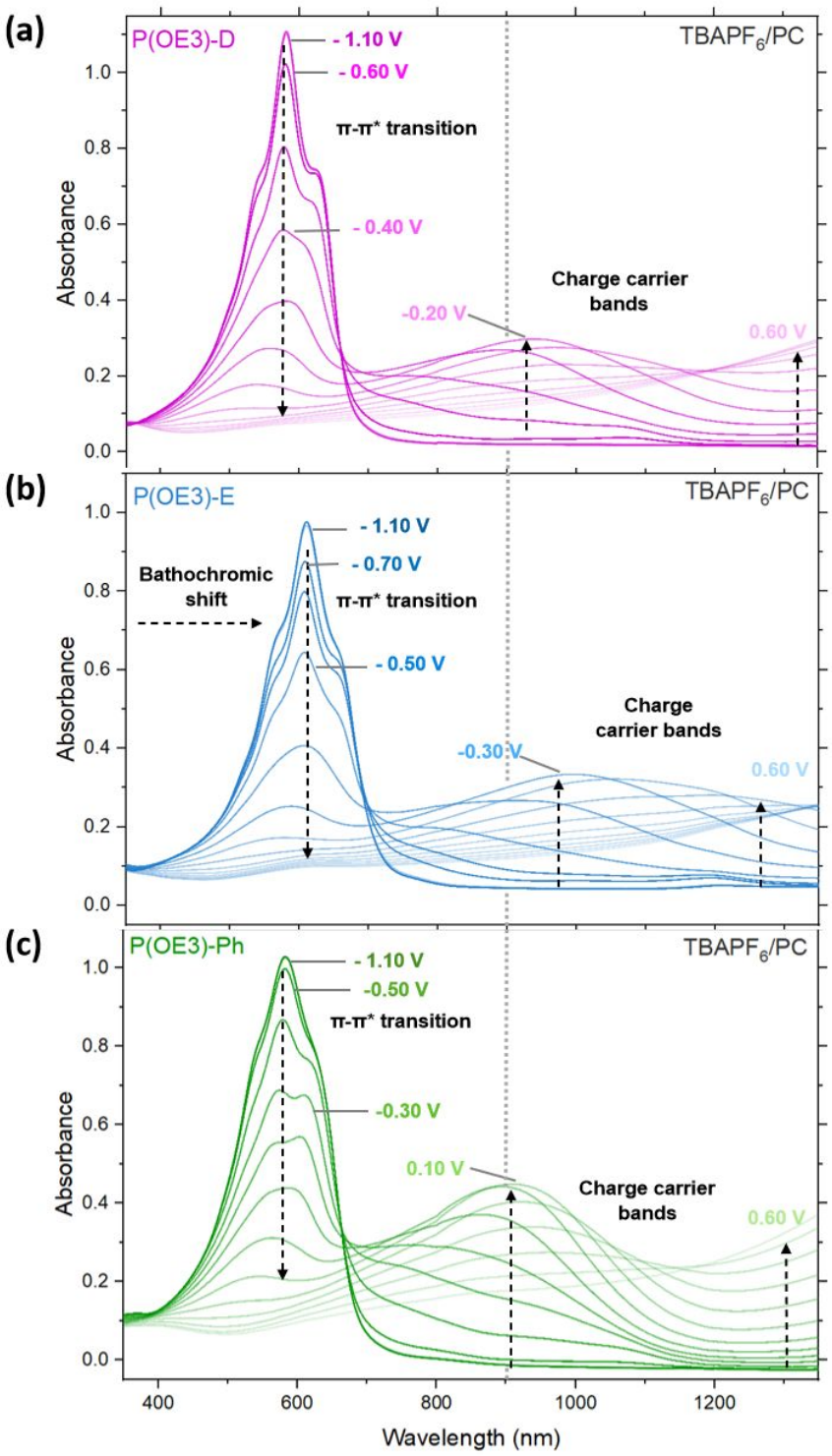

Figure S16. Potential-dependent spectra of (a) P(OE3)-D, (b) P(OE3)-E, (c) P(OE3)-Ph films on ITO/glass recorded every 0.1 V in 0.5 M $TBAPF_6$/PC from -1.1 V to +0.6 V vs. Fc/Fc^+. To aid visualization of higher energy carrier band peaks, a dotted grey line has been dropped at 900 nm.

Table S1. Oxidation Onsets, Theoretical Ionization Energies, Conductance Onsets, and Charge Carrier Band Onsets.

Polymer	$E_{ox,aq}$ vs. Ag/AgCl (V)	$E_{ox,org}$ vs. Fc/Fc^+ (V)	IE_{theor} [a] (eV)	$E_{cond,aq}$ vs. Ag/AgCl (V)	$E_{cond,org}$ vs. Fc/Fc^+ (V)	$E_{charge\ carrier,aq}$ vs. Ag/AgCl (V)	$E_{charge\ carrier,org}$ vs. Fc/Fc^+ (V)
P(OE3)-D	-0.20	-0.59	4.41	+0.20	-0.30	-0.20	-0.60
P(OE3)-E	-0.40	-0.74	4.30	-0.20	-0.50	-0.40	-0.70
P(OE3)-Ph	-0.10	-0.56	4.57	+0.10	-0.30	-0.10	-0.50

[a]IE calculated as the difference in electronic energy of a radical cation and neutral state of a representative dodecamer structure.

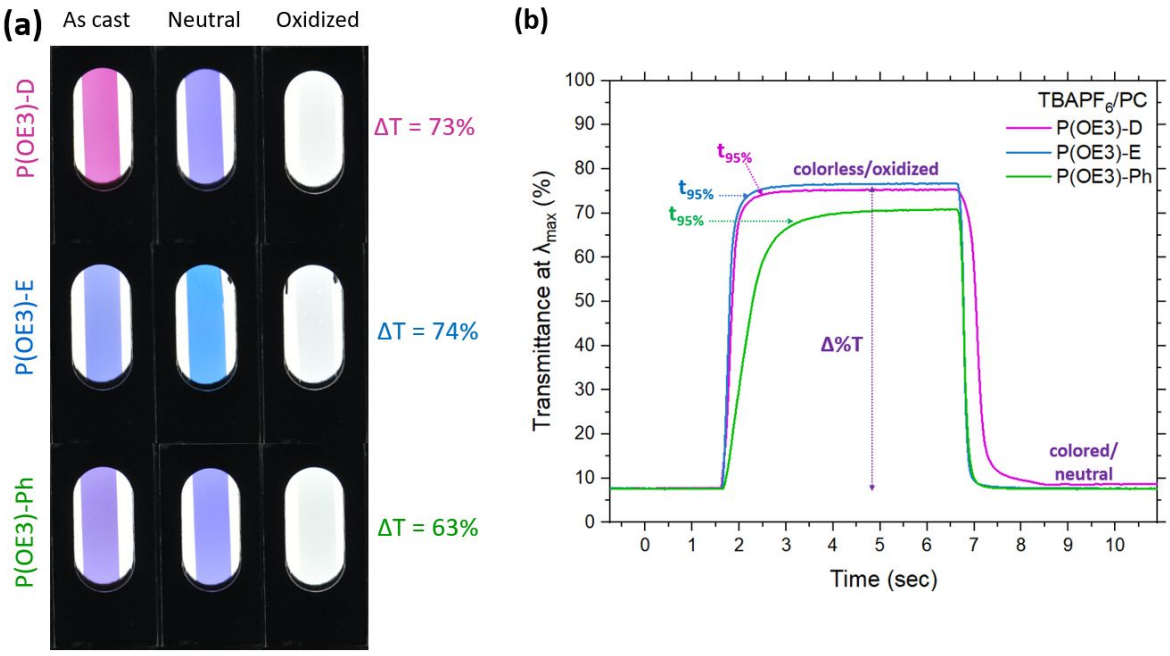

Figure S17. (a) Photographs of spray-cast P(OE3) series films in their as-cast, charge neutral (after electrochemical conditioning), and oxidized states on ITO/glass in a three-electrode cell setup in a quartz cuvette using a Pt flag as a counter electrode and 0.5 M $TBAPF_6$/PC as the electrolyte. (b) Monitoring transmittance at λ_{max} of P(OE3) series with bleaching switching speed to 95% contrast ($t_{95\%}$) indicated in plot.

CIE standard illuminant D50 analysis of L*a*b* color space

By analyzing the colorimetric properties of these copolymer films using the *L*a*b** color space, we can better understand the color evolution as a function of applied potential during the oxidation process. As seen in in **Figure S18a**, after the spray cast films are repeatedly electrochemically switched, the color coordinates for the charge neutral sate are modified from the as-cast pristine states as the polymer chains reorganize, leading to a change in absorbance and perceived color for P(OE3)-E and P(OE3)-D. For P(OE3)-E, the *b** (yellow/blue component) value increases (increased yellow and decreased blue color) and *a** (red/green component) value decreases (decreased red and increased green color). For P(OE3)-D, the *b** value decreases (decreased yellow and increased blue color), and *a** value decreases (decreased red and increased green color). No color change is observed for in P(OE3)-Ph when going from a pristine film to an electrochemically conditioned film in NaCl/H_2O.

The P(OE3) polymers' *L*a*b** are also evaluated for switching in TBAPF$_6$/PC (**Figure S19a**), where similar trends are demonstrated for P(OE3)-E and P(OE3)-D. In general, we note that the changes in color coordinates from as-cast state to electrochemically cycled are significantly more drastic in the organic electrolyte than the aqueous electrolyte. For P(OE3)-Ph in organic electrolyte, the *b** and *a** values decrease slightly for both.

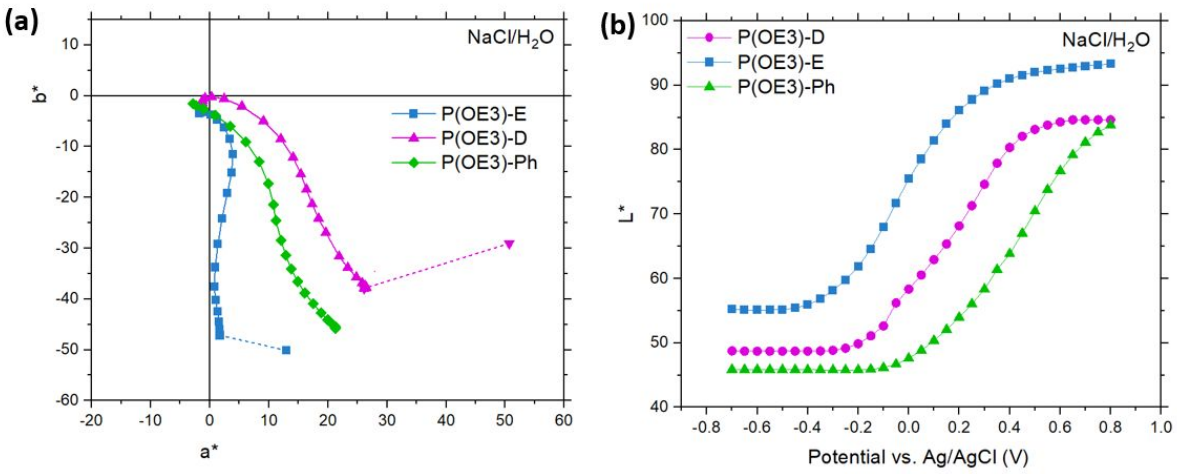

Figure S18. (a) *a*b** diagram showing the color change occurring during electrochemical oxidation of the copolymers from the as-cast films to the charge neutral states after conditioning (dotted lines) and charge neutral to oxidized states (solid lines) in 0.1 V increments. (b) Changes in *L** as a function of potential on ITO/glass in 0.5 M NaCl/ H_2O vs. Ag/AgCl.

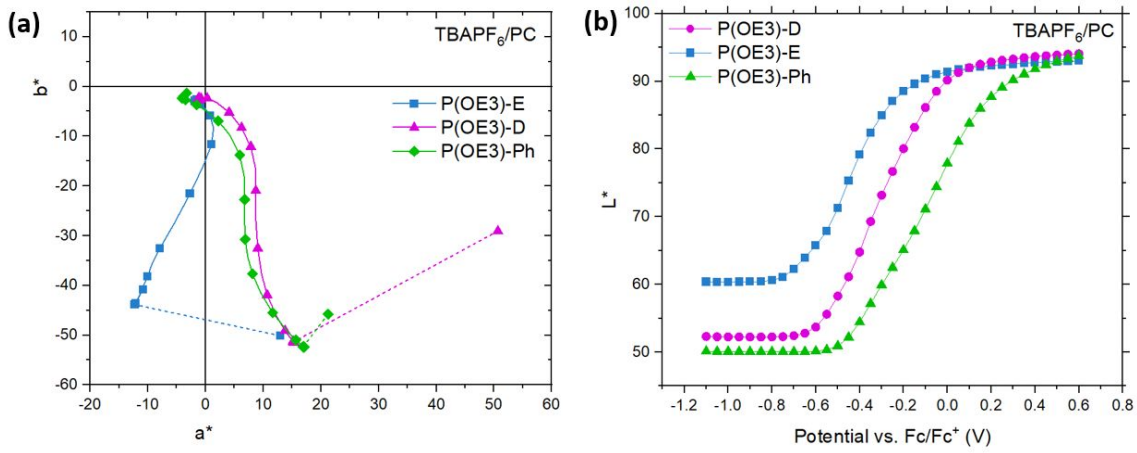

Figure S19. (a) *a*b** diagram showing the color change occurring during electrochemical oxidation of the copolymers from the as-cast films to the charge neutral states after conditioning (dotted lines) and charge neutral to oxidized states (solid lines) in 0.1 V increments. (b) Changes in *L** as a function of potential on ITO/glass in and 0.5 $TBAPF_6$ /PC vs. Fc/Fc^+.

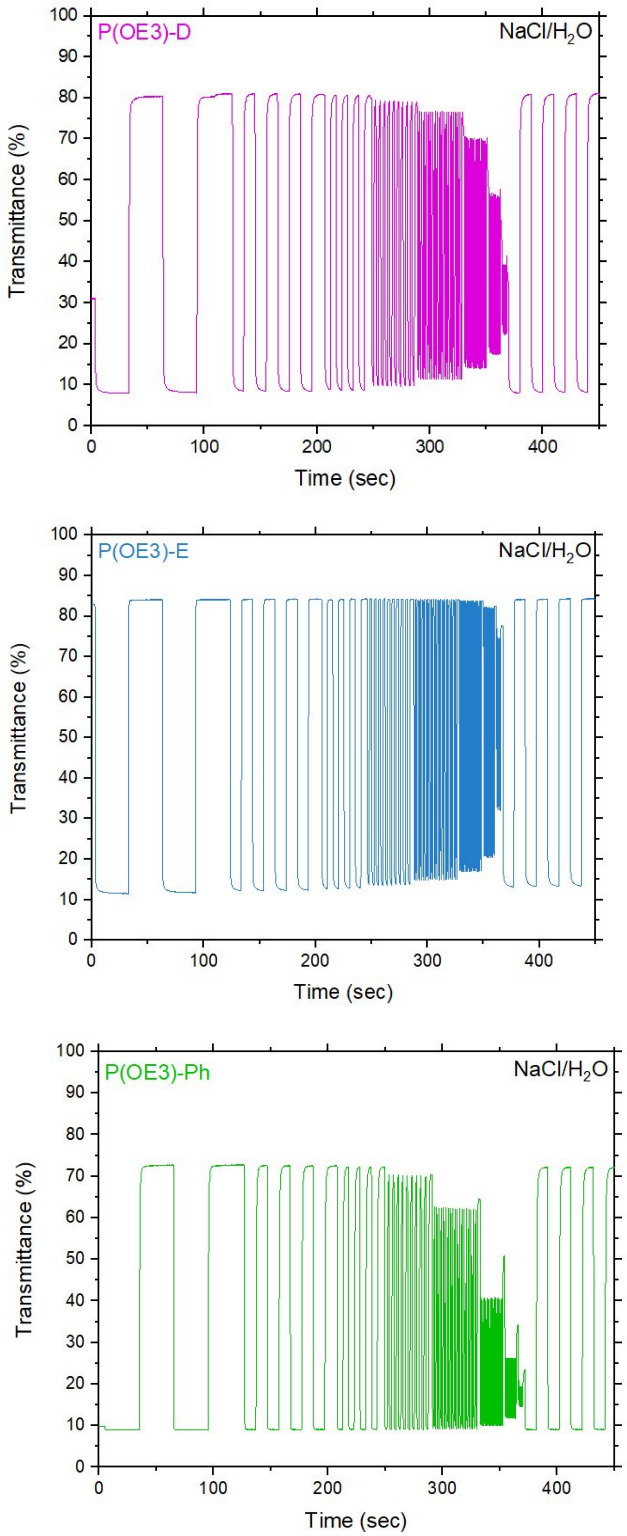

Figure S20. Switching kinetics of polymers at 30, 10, 5, 2, 1, 0.5, 0.25, and 0.1 seconds. Transmittance monitored at λ_{max}. Films switched on ITO/glass in a three-electrode cell setup in a quartz cuvette using a Pt flag as a counter electrode and 0.5 M NaCl/H_2O as the electrolyte from -0.7 to +0.8 V vs. Ag/AgCl.

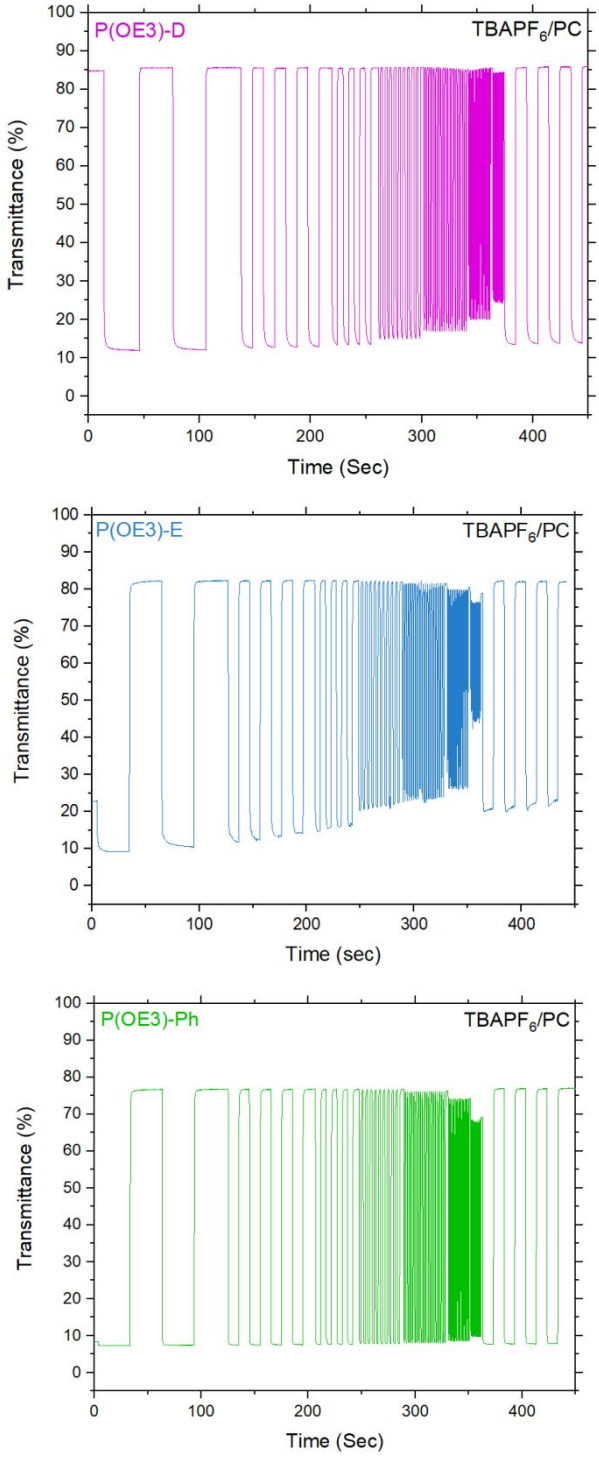

Figure S21. Switching kinetics of polymers at 30, 10, 5, 2, 1, 0.5, and 0.25 second. Transmittance monitored at λ_{max}. Films on ITO/glass in a three-electrode cell setup in a quartz cuvette using a Pt flag as a counter electrode and 0.5 M $TBAPF_6$/PC as the electrolyte from -1.1 V to +0.6 V vs. Fc/Fc^+.

Time Constant (τ) Evaluation

Optical switching is analyzed in two ways: (1) switching speed to 95% coloration or bleaching and (2) a time constant (τ) extracted from an exponential decay function.[14] We report both because the percent coloration or bleaching to which switching speed is reported can vary (*e.g.*, 50, 60, 66, 70, to 80%). τ, which corresponds to 63% of a full transmittance switch, can be used to calculate switching times for any other percentage of a full switch, facilitating comparisons of the P(OE3) family with switching speeds in other systems. To extract τ, an exponential function (**Equation S2**) is fitted to the loss in contrast as a function of pulse time (t).

$$\Delta T(t) = \Delta T_{max}(1 - e^{-\frac{t}{\tau}})$$

Equation S2. The time constant equation.

Partial delamination of the P(OE3)-E film on ITO was observed upon repeated cycling in $TBAPF_6$/PC, explaining this polymer's irreversible loss in switching contrast (**Figure S21**) and poor fit to the time constant equation (**Figure S23**). As such, a reliable τ value could not be calculated for P(OE3)-E in $TBAPF_6$/PC.

Table S2. Optical switching speed ($t_{95\%}$) on the copolymer series in 0.5 M $TBAPF_6$/PC.

Polymer	Switching speed$_{org,\ bleaching}$ (s)	Switching speed$_{org,\ coloration}$ (s)	Organic τ
P(OE3)-D	0.8	1.1	0.15
P(OE3)-E	0.5	0.3	~
P(OE3)-Ph	1.7	0.3	0.13

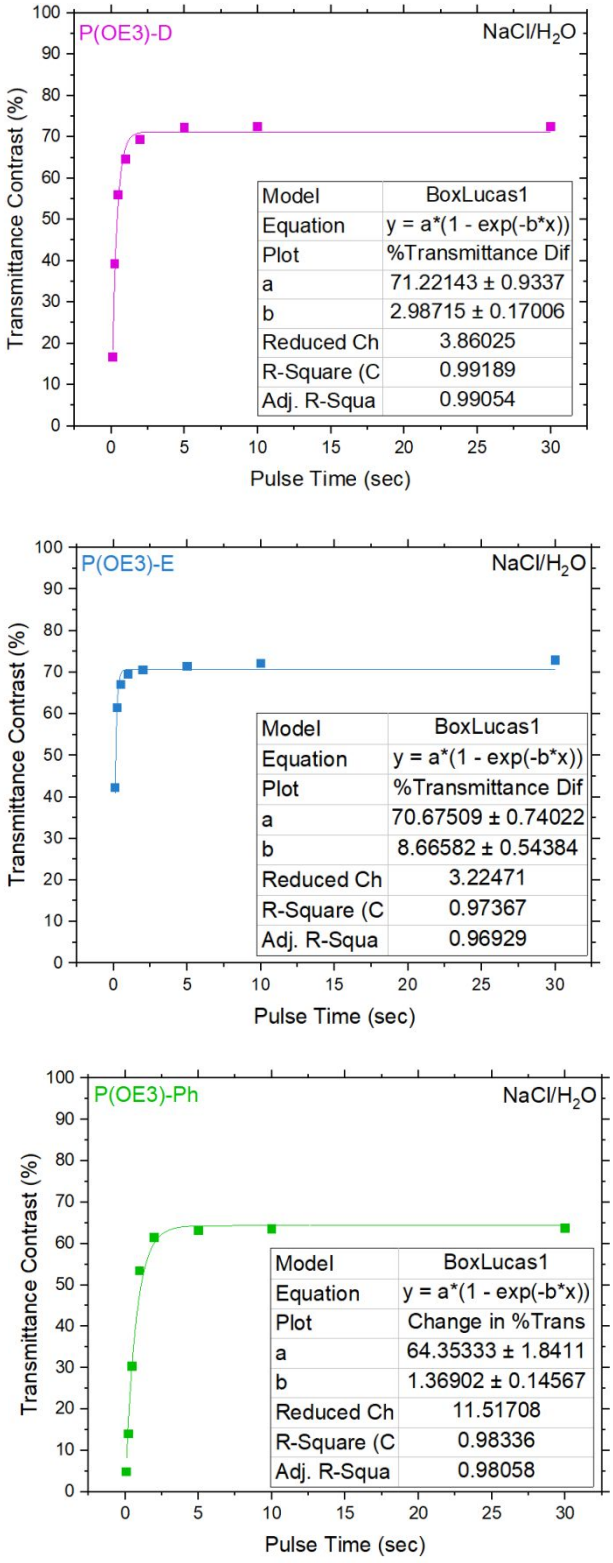

Figure S22. Contrast data extracted from chronoabsorptometry plotted against pulse time to extract the time constant, τ, for switching of P(OE3) films in 0.5 M NaCl/H_2O.

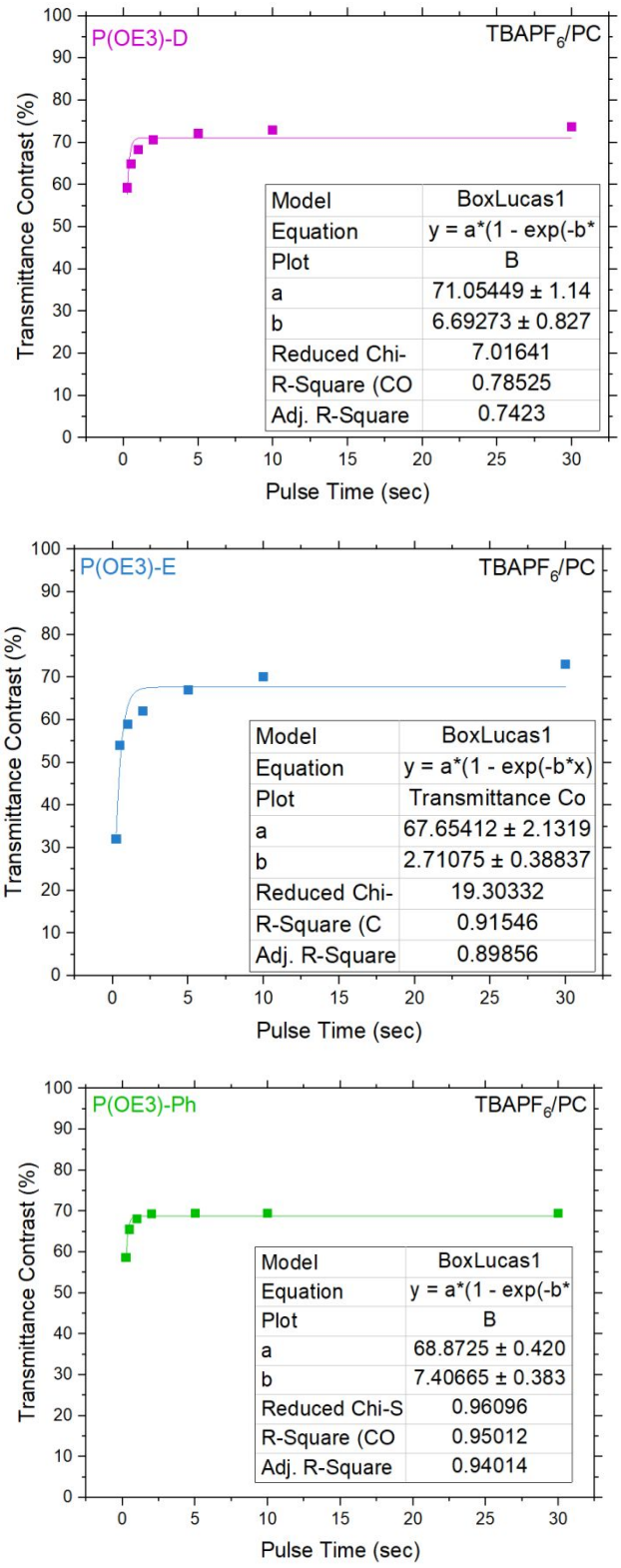

Figure S23. Contrast data extracted from chronoabsorptometry plotted against pulse time to extract the time constant, τ, for switching of P(OE3) films in 0.5 M $TBAPF_6$/PC.

Type I Supercapacitors

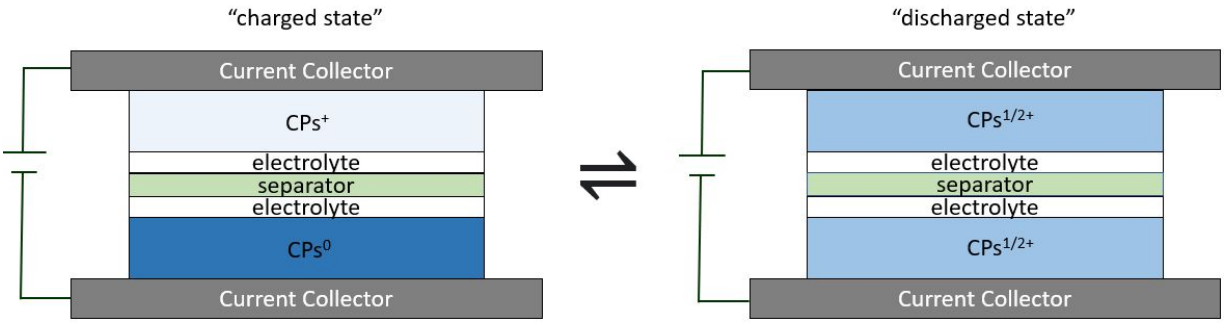

Figure S24. Schematic of Type I supercapacitor in the charged state on the left and discharged state on the right.

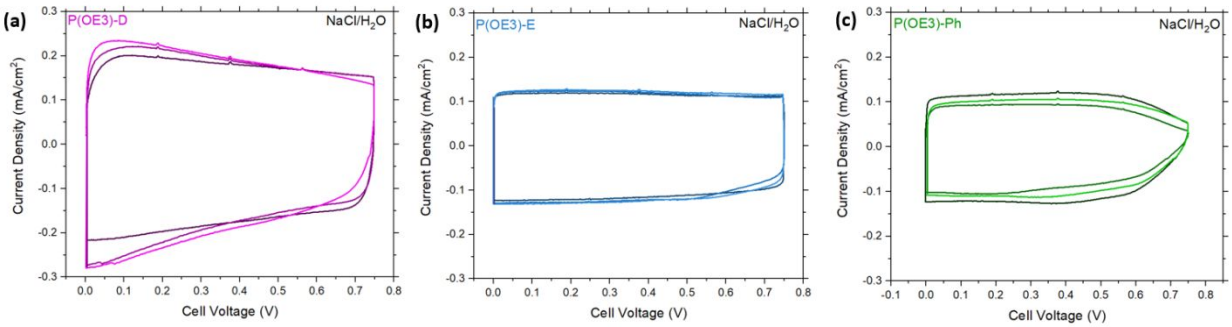

Figure S25. Cyclic voltammograms of three identical devices fabricated with (a) P(OE3)-D, (b) P(OE3)-E, and (c) P(OE3)-Ph as the active layers. All devices operated with 0.5 M $NaCl/H_2O$ as the electrolyte and glassy carbon as the current collector.

References:

(1) Savagian, L. R.; Österholm, A. M.; Ponder, J. F.; Barth, K. J.; Rivnay, J.; Reynolds, J. R. Balancing Charge Storage and Mobility in an Oligo(Ether) Functionalized Dioxythiophene Copolymer for Organic- and Aqueous- Based Electrochemical Devices and Transistors. *Adv. Mater.* **2018**, *30*, 1804647. https://doi.org/10.1002/adma.201804647.

(2) Perepichka, I. F.; Roquet, S.; Leriche, P.; Raimimdo, J. M.; Frère, P.; Roncali, J. Electronic Properties and Reactivity of Short-Chain Oligomers of 3,4-Phenylenedioxythiophene (PheDOT). *Chem. Eur. J.* **2006**, *12* (11), 2960–2966. https://doi.org/10.1002/chem.200501284.

(3) Hou, J.; Park, M. H.; Zhang, S.; Yao, Y.; Chen, L. M.; Li, J. H.; Yang. Bandgap and Molecular Energy Level Control of Conjugated Polymer Photovoltaic Materials Based on Benzo[l,2-b:4,5-B′]Dithiophene. *Macromolecules* **2008**, *41* (16), 6012–6018. https://doi.org/10.1021/ma800820r.

(4) Gomez, E.D.; Weisen, A. E. Densities of Conjugated Polymers as a Function of Temperature https://scholarsphere.psu.edu/resources/f7b9e04f-436e-4b3f-84f6-f5b8f8985221 (accessed 2021 -12 -03).

(5) Österholm, A. M.; Ponder, J. F.; de Keersmaecker, M.; Shen, D. E.; Reynolds, J. R. Disentangling Redox Properties and Capacitance in Solution-Processed Conjugated Polymers. *Chem. Mater.* **2019**, *31* (8), 2971–2982. https://doi.org/10.1021/acs.chemmater.9b00528.

(6) Salinas, G.; Frontana-Uribe, B. A. Analysis of Conjugated Polymers Conductivity by in Situ Electrochemical-Conductance Method. *ChemElectroChem* **2019**, *6* (16), 4105–4117. https://doi.org/10.1002/celc.201801488.

(7) Höök, F.; Rodahl, M.; Brzezinski, P.; Kasemo, B. Energy Dissipation Kinetics for Protein and Antibody-Antigen Adsorption under Shear Oscillation on a Quartz Crystal Microbalance. *Langmuir* **1998**, *14* (4), 729–734. https://doi.org/10.1021/la970815u.

(8) Easley, A. D.; Ma, T.; Eneh, C. I.; Yun, J.; Thakur, R. M.; Lutkenhaus, J. L. A Practical Guide to Quartz Crystal Microbalance with Dissipation Monitoring of Thin Polymer Films. *J. Polym. Sci.* **2021**, 1–18. https://doi.org/10.1002/pol.20210324.

(9) Lee, H. S.; Yee, M. Q.; Eckmann, Y. Y.; Hickok, N. J.; Eckmann, D. M.; Composto, R. J. Reversible Swelling of Chitosan and Quaternary Ammonium Modified Chitosan Brush Layers: Effects of PH and Counter Anion Size and Functionality. *J. Mater. Chem.* **2012**, *22* (37), 19605–19616. https://doi.org/10.1039/c2jm34316a.

(10) Frisch, M. J. et al. Gaussian 16, Revision A.03. Gaussian, Inc.: Wallingford, CT 2016.

(11) Bryan, A. M.; Santino, L. M.; Lu, Y.; Acharya, S.; D'Arcy, J. M. Conducting Polymers for Pseudocapacitive Energy Storage. *Chem. Mater.* **2016**, *28* (17), 5989–5998. https://doi.org/10.1021/acs.chemmater.6b01762.

(12) Glendening, E. D.; Landis, C. R.; Weinhold, F. NBO 6.0: Natural Bond Orbital Analysis Program. *J. Comput. Chem.* **2013**, *34* (16), 1429–1437. https://doi.org/10.1002/jcc.23266.

(13) Moser, M.; Thorley, K. J.; Moruzzi, F.; Ponder, J. F.; Maria, I. P.; Giovannitti, A.; Inal, S.; McCulloch, I. Highly Selective Chromoionophores for Ratiometric Na+ Sensing Based on an

Oligoethyleneglycol Bridged Bithiophene Detection Unit. *J. Mater. Chem. C* **2019**, *7* (18), 5359–5365. https://doi.org/10.1039/c8tc06000b.

(14) Hassab, S.; Shen, D. E.; Österholm, A. M.; da Rocha, M.; Song, G.; Alesanco, Y.; Viñuales, A.; Rougier, A.; Reynolds, J. R.; Padilla, J. A New Standard Method to Calculate Electrochromic Switching Time. *Sol. Energy Mater. Sol. Cells* **2018**, *185*, 54–60. https://doi.org/10.1016/j.solmat.2018.04.031.